Global Practical Tracking for a Hovercraft with Unmeasured Linear Velocity and Disturbances

Wei Xie * **David Cabecinhas** *,** **Rita Cunha** ** **Carlos Silvestre** *,**

* *Faculty of Science and Technology, University of Macau, Macau, China*
(e-mail: {weixie, csilvestre}@ um.edu.mo).
** *Institute for Systems and Robotics, Instituto Superior Técnico,*
Universidade de Lisboa, 1049-001 Lisboa, Portugal
(e-mail: {dcabecinhas, rita}@isr.ist.utl.pt).

Abstract: This paper addresses the design and experimental validation of a trajectory tracking controller for an underactuated hovercraft with unmeasured linear velocity and subject to time-varying disturbances. The unmeasured linear velocity and disturbances are recovered by designing nonlinear observers. A control law is proposed that, in closed-loop with the velocity and disturbance observers, can robustly steer the hovercraft toward and stay within a neighborhood of a reference trajectory. To demonstrate the performance and robustness of the proposed control strategy, we present and analyze experimental results obtained with a model-scale hovercraft.

Keywords: Nonlinear control, robust control, underactuated hovercraft, observers.

1. INTRODUCTION

In the past few years, motion control of underactuated surface vehicles (USVs) has received sustained attention from the control community due to their increasing application in both military and civilian areas. To name a few, USVs can be used for surveillance, border patrolling, ocean exploration, and transportation. In this paper, an underactuated hovercraft, as shown in Fig. 1, is chosen as our study model. This vehicle poses interesting control challenges due to its nonholonomic nature and existence of side-slip, while at the same time being versatile and able to glide effortlessly in a number of different surfaces.

Fig. 1. Underactuated hovercraft with attached markers.

Many nonlinear control strategies for stabilizing USVs have been reported. For example, in Reyhanoglu (1997), the authors proposed a time-invariant discontinuous feedback control law which was able to asymptotically stabilize the system to the

desired trajectory with exponential convergence rate. In Aguiar et al. (2003), a continuous tracking controller was developed to drive an underactuated hovercraft to an arbitrarily small neighborhood of a reference trajectory. Based on a double integrator system, in Cabecinhas and Silvestre (2019), a nonlinear controller was designed to steer an autonomous surface vessel to track a reference trajectory. However, the aforementioned works did not take into account model uncertainties or environmental disturbances in their proposed control strategies. To enhance the robust performance of the controller, Li et al. (2009) used feedback dominance technique to deal with model uncertainties of marine surface vessels, and a pre-filter based sliding mode controller for the nonlinear vessel steering system was proposed in Perera and Soares (2012). Time-invariant disturbance and damping coefficients estimators were designed in Xie et al. (2019) and Lu et al. (2019), while in Cabecinhas et al. (2018) a Kalman filter was applied to estimate unknown vehicle parameters with application to a hovercraft. In Belleter et al. (2019), the authors designed an ocean current estimator to compensate for constant current. A similar method was used in Yin and Xiao (2017), where parameters estimators were designed to estimate unknown constant parameters. Yang et al. (2014) constructed an observer to provide an estimation of unknown time-varying disturbances, ensuring that all the signals of the closed-loop trajectory tracking control system of ships were globally uniformly ultimately bounded. In all these works the full state of the vehicle is assumed to be known.

To cope with unmeasured velocities, in Grovlen and Fossen (1996), a nonlinear observer was designed to estimate linear and angular velocities by using the position and orientation information. In Do and Pan (2006), a high-gain observer was designed to estimate the velocities. However, the estimation methods proposed therein did not consider disturbances. In light of this limitation, Loueipour et al. (2015) proposed a structure for the estimation of low-frequency (LF) and wave-frequency motion components, LF disturbance forces, and vehicles veloc-

ities based on the measured position signals, achieving globally exponentially stability. In Liu et al. (2019), nonlinear extended state observers were proposed, where both linear and angular velocities and disturbances can be recovered by utilizing the position-heading information, under the assumption that the angular velocity of the vehicle is bounded by a specific value. In Zhao and Guo (2015), the authors designed an extended state observer for generic nonlinear systems with uncertainty.

Motivated by the aforementioned studies, in this paper, we propose a nonlinear trajectory tracking controller for an underactuated hovercraft, achieving global practical stability. Linear velocity and disturbances observers are designed to recover the unmeasured linear velocity and estimate the disturbances. Experimental results are presented to validate the performance of the proposed controller. In our recent work Xie et al. (2019), the linear velocity was measurable and only constant disturbances were considered. This paper proposes a solution to the trajectory tracking problem when linear velocity measurement is not available and allows for time-varying disturbances.

The remainder of this paper is structured as follows. Section 2 introduces the notation used throughout the paper. Section 3 shows the vehicle models and control problem statement. Observer and controller design are given in Section 4 and Section 5, respectively. To demonstrate the efficiency of the control methodology, experimental results are presented in Section 6. Finally, Section 7 summarizes the contents of this paper.

2. NOTATION

Throughout this paper, $\mathbb{R}^n$ denotes the n-dimensional Euclidean space. A function f is of class C^n if the derivatives $f', f'', \ldots, f^{(n)}$ exist and are continuous. For a vector $\mathbf{x} \in \mathbb{R}^n$, its estimate is denoted by $\hat{\mathbf{x}}$, with the estimation error $\tilde{\mathbf{x}} = \hat{\mathbf{x}} - \mathbf{x}$. The initial values of $\hat{\mathbf{x}}$ and $\mathbf{x}$ are presented by $\hat{\mathbf{x}}(0)$ and $\mathbf{x}(0)$, respectively. The unit vectors $\mathbf{u}_1$ and $\mathbf{u}_2$ are introduced as $\mathbf{u}_1 = [1\ 0]^\top, \mathbf{u}_2 = [0\ 1]^\top$, $\mathbf{I}_{n \times n}$ is the identity matrix, $\mathbf{0}_{m \times n}$ is a matrix whose elements are zero. For the reader's reference, Table 1 summarizes some main symbols and their corresponding descriptions used in the follows.

Table 1. Symbols summary

$\{I\}, \{B\}$	inertial frame and body frame
$\mathbf{p}$	hovercraft's position expressed in $\{I\}$
ψ	hovercraft's orientation
$\mathbf{R}$	rotation matrix from $\{B\}$ to $\{I\}$
$\mathbf{v}$	linear velocity expressed in $\{I\}$
ω	angular velocity
m, J	hovercraft's mass and moment of inertia
T, τ	thrust and torque inputs
$\mathbf{f}_v, f_\omega$	disturbances
k_1, k_2, k_3	positive control gains
$\lambda_v, \lambda_\omega, \zeta_v, \zeta_\omega$	positive estimation gains

3. PROBLEM FORMULATION

This section starts by exposing the kinematic and dynamic models of an underactuated hovercraft, and follows with a formulation of the trajectory tracking problem.

3.1 Hovercraft Model

Define a fixed inertial frame $\{I\}$ and a body frame $\{B\}$ attached to the hovercraft's center of mass, as shown in Fig. 2. The kinematic equations of the hovercraft are written as
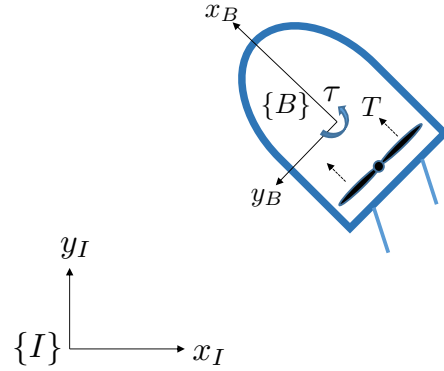

Fig. 2. Sketch of a hovercraft.

$$\begin{aligned} \dot{\mathbf{p}} &= \mathbf{v} \\ \dot{\psi} &= \omega \end{aligned} \tag{1}$$

and the dynamic equations are given as

$$\begin{aligned} \dot{\mathbf{v}} &= m^{-1} T \mathbf{R} \mathbf{u}_1 + \mathbf{f}_v \\ \dot{\omega} &= J^{-1} \tau + f_\omega \end{aligned} \tag{2}$$

where $\mathbf{p} \in \mathbb{R}^2$ is the coordinate of the hovercraft's center of mass, expressed in the inertial frame $\{I\}$, and $\psi \in \mathbb{R}$ denotes the orientation of the hovercraft. The vector $\mathbf{v} \in \mathbb{R}^2$ denotes the linear velocity, expressed in the inertial frame $\{I\}$ while $\omega \in \mathbb{R}$ is the angular velocity, expressed in the body frame $\{B\}$. The rotation matrix from $\{B\}$ to $\{I\}$ is denoted by $\mathbf{R}$, satisfying $\dot{\mathbf{R}} = \mathbf{R}\mathbf{S}\omega$. with

$$\mathbf{R} = \begin{bmatrix} \cos(\psi) & -\sin(\psi) \\ \sin(\psi) & \cos(\psi) \end{bmatrix}, \quad \mathbf{S} = \begin{bmatrix} 0 & -1 \\ 1 & 0 \end{bmatrix}.$$

The thrust force T and torque τ are inputs. The vehicle's mass and moment of inertia are denoted by m and J, respectively. Disturbances are represented by $\mathbf{f}_v$ and f_ω. The model also makes the following assumptions.

Assumption 1. The vehicle states $\mathbf{p}, \psi, \omega$ are measurable, but the linear velocity $\mathbf{v}$ is not.

Assumption 2. The disturbances $\mathbf{f}_v$ and f_ω are unknown, time-varying, and satisfy

$$\|\dot{\mathbf{f}}_v\| \le \overline{f}_v, |\dot{f}_\omega| \le \overline{f}_\omega$$

with $\overline{f}_v, \overline{f}_\omega$ are known.

3.2 Problem Statement

The trajectory tracking problem with unknown linear velocity and disturbances is stated as follows. Let the reference trajectory $\mathbf{p}_d(t) \in \mathbb{R}^2$ be a curve of class at least C^4, whose time derivatives are bounded. The control objective is to design control law for T and τ, linear velocity and disturbances observers, such that the vehicle can be steered to an arbitrarily small neighborhood of $\mathbf{p}_d(t)$.

4. OBSERVER DESIGN

In this section, we present nonlinear observers to recover unmeasured linear velocity and unknown disturbances. Inspired by the nonlinear extended state observer presented in Liu et al. (2019), observers for $\mathbf{v}, \mathbf{f}_v$ and f_ω are designed as follows,

$$\dot{\hat{\mathbf{p}}} = -a\lambda_v \tilde{\mathbf{p}} + \hat{\mathbf{v}}$$
$$\dot{\hat{\mathbf{v}}} = -a\lambda_v^2 \tilde{\mathbf{p}} + \hat{\mathbf{f}}_v + m^{-1}T\mathbf{R}\mathbf{u}_1 \qquad (3)$$
$$\dot{\hat{\mathbf{f}}}_v = -\lambda_v^3 \tilde{\mathbf{p}}$$

and

$$\dot{\hat{\psi}} = -b\lambda_\omega \tilde{\psi} + \hat{\omega}$$
$$\dot{\hat{\omega}} = -b\lambda_\omega^2 \tilde{\psi} + \hat{f}_\omega + J^{-1}\tau \qquad (4)$$
$$\dot{\hat{f}}_\omega = -\lambda_\omega^3 \tilde{\psi}$$

where $a \geq 3, b \geq 3, \lambda_v > 0, \lambda_\omega > 0$ are estimate gains.

Theorem 1. Consider the designed observers (3)-(4), and the error dynamics

$$\dot{\mathbf{z}}_v = -\lambda_v \mathbf{A}_v \mathbf{z}_v + \mathbf{B}_v \dot{\mathbf{f}}_v, \quad \dot{\mathbf{z}}_\omega = -\lambda_\omega \mathbf{A}_\omega \mathbf{z}_\omega + \mathbf{B}_\omega \dot{f}_\omega$$

where $\mathbf{z}_v = [\mathbf{z}_{v1}^\top, \mathbf{z}_{v2}^\top, \mathbf{z}_{v2}^\top]^\top, \mathbf{z}_\omega = [z_{\omega1}, z_{\omega2}, z_{\omega3}]^\top, \mathbf{z}_{v1} = \lambda_v^2 \tilde{\mathbf{p}}, \mathbf{z}_{v2} = \lambda_v \tilde{\mathbf{v}}, \mathbf{z}_{v3} = \tilde{\mathbf{f}}_v, z_{\omega1} = \lambda_\omega^2 \tilde{\psi}, z_{\omega2} = \lambda_\omega \tilde{\omega}, z_{\omega3} = \tilde{f}_\omega,$

$$\mathbf{A}_v = \begin{bmatrix} a\mathbf{I}_{2\times2} & -\mathbf{I}_{2\times2} & \mathbf{0}_{2\times2} \\ a\mathbf{I}_{2\times2} & \mathbf{0}_{2\times2} & -\mathbf{I}_{2\times2} \\ \mathbf{I}_{2\times2} & \mathbf{0}_{2\times2} & \mathbf{0}_{2\times2} \end{bmatrix}, \quad \mathbf{B}_v = \begin{bmatrix} \mathbf{0}_{2\times2} \\ \mathbf{0}_{2\times2} \\ -\mathbf{I}_{2\times2} \end{bmatrix}$$

and

$$\mathbf{A}_\omega = \begin{bmatrix} b & -1 & 0 \\ b & 0 & -1 \\ 1 & 0 & 0 \end{bmatrix}, \quad \mathbf{B}_\omega = \begin{bmatrix} 0 \\ 0 \\ -1 \end{bmatrix}.$$

For $a \geq 3, b \geq 3, \lambda_v > 0, \lambda_\omega > 0$, $\mathbf{z}_v$ and $\mathbf{z}_\omega$ converge each to a ball centered at the origin, whose radius depends on $\lambda_v, \lambda_\omega$ and can be rendered arbitrarily small.

Proof: The eigenvalues of $\mathbf{A}_v$ are given as

$$E_v = \left\{1, (a-1)/2 \pm \sqrt{(a+1)(a-3)}/2\right\}$$

which are positive for $a \geq 3$. Now we define a Lyapunov candidate function as

$$V_v = \frac{1}{2}\mathbf{z}_v^\top \mathbf{z}_v.$$

Computing its time derivative, we have

$$\dot{V}_v = -\lambda_v \mathbf{z}_v^\top \mathbf{A}_v \mathbf{z}_v + \mathbf{z}_v^\top \mathbf{B}_v \dot{\mathbf{f}}_v$$
$$\leq -\|\mathbf{z}_v\|\left(\lambda_v \lambda_{\min}(E_v)\|\mathbf{z}_v\| - \overline{f}_v\right)$$

which is strictly negative definite for $\|\mathbf{z}_v\| > \overline{f}_v\left(\lambda_v \lambda_{\min}(E_v)\right)^{-1}$, where $\lambda_{\min}(E_v)$ denotes the minimum eigenvalue of E_v,

$$\lambda_{\min}(E_v) = \min\left\{1, (a-1)/2 - \sqrt{(a+1)(a-3)}/2\right\}. \quad (5)$$

It follows that $\|\mathbf{z}_v\| = (\lambda_v^4\|\tilde{\mathbf{p}}\|^2 + \lambda_v^2\|\tilde{\mathbf{v}}\|^2 + \|\tilde{\mathbf{f}}_v\|^2)^{\frac{1}{2}}$ is uniformly ultimately bounded by $\overline{f}_v\left(\lambda_v \lambda_{\min}(E_v)\right)^{-1}$ which can be made arbitrarily small by increasing λ_v. Notice that for constant disturbances, we have $\overline{f}_v = 0$. In this case, $\mathbf{z}_v$ will be driven to zero as time goes to infinity. Similarly, we can prove $\mathbf{z}_\omega$ converges to an arbitrarily small ball centered at the origin.

Remark 1. For fixed $\lambda_v, \overline{f}_v$, the larger $\lambda_{\min}(E_v)$ is, the smaller $\overline{f}_v\left(\lambda_v \lambda_{\min}(E_v)\right)^{-1}$. To make $\lambda_{\min}(E_v)$ as large as possible, we go back to $\lambda_{\min}(E_v)$, as defined in (5). From where it can be obtained that

$$(a-1)/2 - \sqrt{(a+1)(a-3)}/2 \leq 1, \text{for } a \geq 3$$

holds. As a result, the maximum value of $\lambda_{\min}(E_v)$ is

$$\max_a\{\lambda_{\min}(E_v)\} = 1, \text{for } a = 3.$$

Similarly, we have the maximum value of $\lambda_{\min}(E_\omega)$ is

$$\max_b\{\lambda_{\min}(E_\omega)\} = 1, \text{for } b = 3$$

where $\lambda_{\min}(E_\omega) = \min\{1, (b-1)/2 - \sqrt{(b+1)(b-3)}/2\}$.

As we established above, for fixed $\lambda_v, \lambda_\omega, \overline{f}_v, \overline{f}_\omega$, only when $a = b = 3$ holds, we obtain the minimum

$$\overline{f}_v\left(\lambda_v \lambda_{\min}(E_v)\right)^{-1}, \overline{f}_\omega\left(\lambda_\omega \lambda_{\min}(E_\omega)\right)^{-1}.$$

In light of this consideration, we choose $a = 3, b = 3$. Then, to reduce the ultimate bounds of the estimate errors $\|\mathbf{z}_v\|, \|\mathbf{z}_\omega\|$, it is necessary to increase $\lambda_v, \lambda_\omega$. However, too large estimate gains $\lambda_v, \lambda_\omega$ could lead to undesired *peaking* phenomenon during the initial transient period, especially for the disturbance estimate. In order to tune the values of $\hat{\mathbf{f}}_v, \hat{f}_\omega$ independently, we introduce two more estimate gains ζ_v, ζ_ω and rewrite the observers as follows,

$$\dot{\hat{\mathbf{p}}} = -3\lambda_v \tilde{\mathbf{p}} + \hat{\mathbf{v}}$$
$$\dot{\hat{\mathbf{v}}} = -3\lambda_v^2 \tilde{\mathbf{p}} + \hat{\mathbf{f}}_v + m^{-1}T\mathbf{R}\mathbf{u}_1 \qquad (6)$$
$$\dot{\hat{\mathbf{f}}}_v = -\zeta_v \lambda_v^3 \tilde{\mathbf{p}}$$

and

$$\dot{\hat{\psi}} = -3\lambda_\omega \tilde{\psi} + \hat{\omega}$$
$$\dot{\hat{\omega}} = -3\lambda_\omega^2 \tilde{\psi} + \hat{f}_\omega + J^{-1}\tau \qquad (7)$$
$$\dot{\hat{f}}_\omega = -\zeta_\omega \lambda_\omega^3 \tilde{\psi}$$

where ζ_v, ζ_ω are positive numbers that will be specified later.

Theorem 2. Consider the designed observers (6)-(7), and the error dynamics

$$\dot{\mathbf{z}}_v = \lambda_v \mathbf{C}_v \mathbf{z}_v + \mathbf{B}_v \dot{\mathbf{f}}_v, \quad \dot{\mathbf{z}}_\omega = \lambda_\omega \mathbf{C}_\omega \mathbf{z}_\omega + \mathbf{B}_\omega \dot{f}_\omega$$

where

$$\mathbf{C}_v = \begin{bmatrix} -3\mathbf{I}_{2\times2} & \mathbf{I}_{2\times2} & \mathbf{0}_{2\times2} \\ -3\mathbf{I}_{2\times2} & \mathbf{0}_{2\times2} & \mathbf{I}_{2\times2} \\ -\zeta_v\mathbf{I}_{2\times2} & \mathbf{0}_{2\times2} & \mathbf{0}_{2\times2} \end{bmatrix}, \quad \mathbf{C}_\omega = \begin{bmatrix} -3 & 1 & 0 \\ -3 & 0 & 1 \\ -\zeta_\omega & 0 & 0 \end{bmatrix}.$$

For $0 < \zeta_v < 9, 0 < \zeta_\omega < 9$, the estimation errors $\mathbf{z}_v$ and $\mathbf{z}_\omega$ converge each to an arbitrarily small ball centered at the origin.

Proof: The eigenvalues of $\mathbf{C}_v$ have the following real parts

$$R_E = \left\{-1 + (1-\zeta_v)^{\frac{1}{3}}, -1 - (1-\zeta_v)^{\frac{1}{3}}/2\right\}$$

where ζ_v is chosen to satisfy $0 < \zeta_v < 9$, such that

$$-1 + (1-\zeta_v)^{\frac{1}{3}} < 0, -1 - (1-\zeta_v)^{\frac{1}{3}}/2 < 0$$

guaranteeing $\mathbf{C}_v$ is Hurwitz. Let $\mathbf{Q}_v$ be a positive definite matrix satisfying

$$\mathbf{C}_v^\top \mathbf{Q}_v + \mathbf{Q}_v \mathbf{C}_v = -\mathbf{I}_{6\times6}.$$

Now we define a Lyapunov candidate function as

$$V_c = \mathbf{z}_v^\top \mathbf{Q}_v \mathbf{z}_v \qquad (8)$$

whose time derivative yields

$$\dot{V}_c \leq \lambda_v \mathbf{z}_v^\top(\mathbf{C}_v^\top\mathbf{Q}_v + \mathbf{Q}_v\mathbf{C}_v)\mathbf{z}_v + \mathbf{z}_v^\top(\mathbf{Q}_v + \mathbf{Q}_v^\top)(\mathbf{B}_v\dot{\mathbf{f}}_v)$$
$$\leq -\|\mathbf{z}_v\|\left(\lambda_v\|\mathbf{z}_v\| - 2\lambda_{\max}(\mathbf{Q}_v)\overline{f}_v\right)$$

which is strictly negative definite for $\|\mathbf{z}_v\| > 2\lambda_{\max}(\mathbf{Q}_v)\overline{f}_v\lambda_v^{-1}$, where $\lambda_{\max}(\mathbf{Q}_v)$ denotes the maximum eigenvalue of $\mathbf{Q}_v$. It can be further obtained that $\mathbf{z}_v$ converges to a ball centered at the origin with radius $2\lambda_{\max}(\mathbf{Q}_v)\overline{f}_v\lambda_v^{-1}$. The same technique can be applied to have $\mathbf{z}_\omega$ converge to an arbitrarily small ball centered at the origin.

5. CONTROLLER DESIGN

In this section, the trajectory tracking problem is solved by following the backstepping technique. We start from a Lyapunov candidate function based on the position error and iterate it until thrust force and torque are obtained.

During the backstepping procedure, the unmeasured linear velocity and disturbances are replaced by their corresponding estimates, guaranteeing that all terms included in the control law are known. The introduction of disturbance observers improves the robust performance of the controller.

We define the position error, in the inertial frame, as

$$\mathbf{z}_1 = \mathbf{p} - \mathbf{p}_d$$

and consider a first Lyapunov candidate function as

$$V_1 = \frac{1}{2}\mathbf{z}_1^\top \mathbf{z}_1$$

whose time derivative yields

$$\dot{V}_1 = -W_1(\mathbf{z}_1) + \mathbf{z}_1^\top \mathbf{R}\big(\mathbf{R}^\top \hat{\mathbf{v}} - \mathbf{R}^\top \dot{\mathbf{p}}_d + k_1 \mathbf{R}^\top \mathbf{z}_1\big) - \mathbf{z}_1^\top \tilde{\mathbf{v}}. \quad (9)$$

where $W_1(\mathbf{z}_1) = k_1 \mathbf{z}_1^\top \mathbf{z}_1$, and k_1 is a positive control gain.

According to Aguiar and Hespanha (2007), a second error $\mathbf{z}_2$, is defined as

$$\mathbf{z}_2 = \mathbf{R}^\top \hat{\mathbf{v}} - \mathbf{R}^\top \dot{\mathbf{p}}_d + k_1 \mathbf{R}^\top \mathbf{z}_1 - \boldsymbol{\delta}$$

where $\boldsymbol{\delta} = [\delta_1, \delta_2]^\top, \delta_1 \neq 0$ is a constant vector. Now we can rewrite (9) as

$$\dot{V}_1 = -W_1(\mathbf{z}_1) + \mathbf{z}_1^\top \mathbf{R}(\mathbf{z}_2 + \boldsymbol{\delta}) - \mathbf{z}_1^\top \tilde{\mathbf{v}}.$$

Following the backstepping procedure, a second Lyapunov candidate function is defined as

$$V_2 = V_1 + \frac{1}{2}\mathbf{z}_2^\top \mathbf{z}_2.$$

Computing its time derivative, we have

$$\dot{V}_2 = -W_2(\mathbf{z}_1, \mathbf{z}_2) + \mathbf{z}_1^\top \mathbf{R}\boldsymbol{\delta} + \mathbf{z}_2^\top \big(-\mathbf{S}\delta\omega + m^{-1}T\mathbf{u}_1 + \mathbf{h}\big) + \Omega_1(\mathbf{z}_1, \mathbf{z}_2, \tilde{\mathbf{p}}, \tilde{\mathbf{v}}) \quad (10)$$

with $W_2(\mathbf{z}_1, \mathbf{z}_2) = W_1(\mathbf{z}_1) + k_2 \mathbf{z}_2^\top \mathbf{z}_2$, k_2 is a positive control gain, $\Omega_1(\mathbf{z}_1, \mathbf{z}_2, \tilde{\mathbf{p}}, \tilde{\mathbf{v}}) = -\mathbf{z}_1^\top \tilde{\mathbf{v}} - \mathbf{z}_2^\top \mathbf{R}^\top (3\lambda_v^2 \tilde{\mathbf{p}} + k_1 \mathbf{R}^\top \tilde{\mathbf{v}})$ and $\mathbf{h} = \mathbf{R}^\top \mathbf{z}_1 + \mathbf{R}^\top \hat{\mathbf{f}}_v - \mathbf{R}^\top \ddot{\mathbf{p}}_d + k_1 \mathbf{R}^\top (\hat{\mathbf{v}} - \dot{\mathbf{p}}_d) + k_2 \mathbf{z}_2$.

To zero out the first component of $(-\mathbf{S}\delta\omega + \mathbf{h})$, we choose the thrust force T, as

$$T = -m(\delta_2 \omega + \mathbf{u}_1^\top \mathbf{h}). \quad (11)$$

Substituting (11) into (10), we have

$$\dot{V}_2 = -W_2(\mathbf{z}_1, \mathbf{z}_2) + \mathbf{z}_1^\top \mathbf{R}\boldsymbol{\delta} + (\mathbf{u}_2^\top \mathbf{z}_2)(\delta_1 \omega + \mathbf{u}_2^\top \mathbf{h}) + \Omega_1(\mathbf{z}_1, \mathbf{z}_2, \tilde{\mathbf{p}}, \tilde{\mathbf{v}}).$$

Continuing with backstepping procedure, a third error, is defined as

$$\mathbf{z}_3 = \delta_1 \omega + \mathbf{u}_2^\top \mathbf{h}$$

Then, $\dot{V}_2$ can be rewritten as

$$\dot{V}_2 = -W_2(\mathbf{z}_1, \mathbf{z}_2) + \mathbf{z}_1^\top \mathbf{R}\boldsymbol{\delta} + (\mathbf{u}_2^\top \mathbf{z}_2)z_3 + \Omega_1(\mathbf{z}_1, \mathbf{z}_2, \tilde{\mathbf{p}}, \tilde{\mathbf{v}}).$$

Define a new Lyapunov candidate function is chosen as

$$V_3 = V_2 + \frac{1}{2}z_3^2 \quad (12)$$

whose time derivative is

$$\dot{V}_3 = -W_3(\mathbf{z}_1, \mathbf{z}_2, z_3) + \mathbf{z}_1^\top \mathbf{R}\boldsymbol{\delta} + z_3\big(\mathbf{u}_2^\top \hat{\mathbf{h}} + k_3 z_3 + \mathbf{u}_2^\top \mathbf{z}_2 - \delta_1(J^{-1}\tau + \hat{f}_\omega)\big) + \Omega_1(\mathbf{z}_1, \mathbf{z}_2, \tilde{\mathbf{p}}, \tilde{\mathbf{v}}) + \Omega_2(z_3, \tilde{\mathbf{p}}, \tilde{\mathbf{v}}, \tilde{f}_\omega) \quad (13)$$

with

$$\hat{\mathbf{h}} = \dot{\mathbf{h}} + \Big(\zeta_v \lambda_v^3 \frac{\partial \mathbf{h}}{\partial \hat{\mathbf{f}}_v} + 3\lambda_v^2 \frac{\partial \mathbf{h}}{\partial \hat{\mathbf{v}}}\Big)\tilde{\mathbf{p}}$$

and

$$\Omega_2(z_3, \tilde{\mathbf{p}}, \tilde{\mathbf{v}}, \tilde{f}_\omega) = z_3 \delta_1 \tilde{f}_\omega + z_3 \mathbf{u}_2^\top \Big(\zeta_v \lambda_v^3 \frac{\partial \mathbf{h}}{\partial \hat{\mathbf{f}}_v} + 3\lambda_v^2 \frac{\partial \mathbf{h}}{\partial \hat{\mathbf{v}}}\Big).$$

To zero out $(\mathbf{u}_2^\top \mathbf{z}_2 - \delta_1(J^{-1}\tau + \hat{f}_\omega) + \mathbf{u}_2^\top \hat{\mathbf{h}} + k_3 z_3)$, we choose τ as

$$\tau = J\delta_1^{-1}(\mathbf{u}_2^\top \hat{\mathbf{h}} + k_3 z_3 + \mathbf{u}_2^\top \mathbf{z}_2) - J\hat{f}_\omega \quad (14)$$

which is always well-defined for $\delta_1 \neq 0$. Substituting (14) into (13), we have

$$\dot{V}_3 = -W_3(\mathbf{z}_1, \mathbf{z}_2, z_3) + \mathbf{z}_1^\top \mathbf{R}\boldsymbol{\delta} + \Omega_1(\mathbf{z}_1, \mathbf{z}_2, \tilde{\mathbf{p}}, \tilde{\mathbf{v}}) + \Omega_2(z_3, \tilde{\mathbf{p}}, \tilde{\mathbf{v}}, \tilde{f}_\omega)$$

where $W_3(\mathbf{z}_1, \mathbf{z}_2, z_3) = W_2(\mathbf{z}_1, \mathbf{z}_2) + k_3 z_3^2$, and k_3 is a positive control gain.

The main result is summarized in the following theorem.

Theorem 3. Let the hovercraft's model be described by (1)-(2), $\mathbf{p}_d \in C^4$ be a reference trajectory with bounded time derivatives. Consider the closed-loop system resulting from application of the control inputs, thrust force (11) and torque (14), observers (6), (7). Then, for any initial position and estimation errors, the error $\mathbf{z} = [\|\mathbf{z}_1\|, \|\mathbf{z}_2\|, \|z_3\|, \|\mathbf{z}_v\|, \|\mathbf{z}_\omega\|]^\top$, converges to an arbitrarily small ball centered at the origin as time goes to infinity.

Proof: To prove the closed-loop system is global practical stable, we define a new Lyapunov candidate function as

$$V_4 = V_3 + V_c + \mathbf{z}_\omega^\top \mathbf{Q}_\omega \mathbf{z}_\omega$$

where V_3 and V_c are defined in (12) and (8), respectively, $\mathbf{Q}_\omega$ is a positive definite matrix satisfying

$$\mathbf{C}_\omega^\top \mathbf{Q}_\omega + \mathbf{Q}_\omega \mathbf{C}_\omega = -\mathbf{I}_{3\times 3}.$$

Computing the time derivative of V_4, in closed-loop, we have

$$\dot{V}_4 \leq -k_1\|\mathbf{z}_1\|^2 - k_2\|\mathbf{z}_2\|^2 - k_3\|z_3\|^2 - \lambda_v\|\mathbf{z}_v\|^2 - \lambda_\omega\|\mathbf{z}_\omega\|^2 + 2\lambda_{\max}(\mathbf{Q}_v)\bar{f}_v\|\mathbf{z}_v\| + 2\lambda_{\max}(\mathbf{Q}_\omega)\bar{f}_\omega\|\mathbf{z}_\omega\| + \|\mathbf{z}_1\|\|\boldsymbol{\delta}\| \quad (15)$$
$$+ \Omega_1(\mathbf{z}_1, \mathbf{z}_2, \tilde{\mathbf{p}}, \tilde{\mathbf{v}}) + \Omega_2(z_3, \tilde{\mathbf{p}}, \tilde{\mathbf{v}}, \tilde{f}_\omega)$$

where

$$\Omega_1(\mathbf{z}_1, \mathbf{z}_2, \tilde{\mathbf{p}}, \tilde{\mathbf{v}}) = \Omega_1(\mathbf{z}_1, \mathbf{z}_2, \lambda_v^{-2}\mathbf{z}_{v1}, \lambda_v^{-1}\mathbf{z}_{v2})$$
$$= -\mathbf{z}_1^\top \mathbf{z}_{v2}\lambda_v^{-1} - \mathbf{z}_2^\top \mathbf{R}^\top(3\mathbf{z}_{v1} + k_1\lambda_v^{-1}\mathbf{z}_{v2})$$
$$\leq \lambda_v^{-1}\big(\epsilon\|\mathbf{z}_1\|^2 + \|\mathbf{z}_v\|^2(4\epsilon)^{-1}\big) + 3\big(\epsilon\|\mathbf{z}_2\|^2 + \|\mathbf{z}_v\|(4\epsilon)^{-1}\big)$$
$$+ k_1\lambda_v^{-1}\big(\epsilon\|\mathbf{z}_2\|^2 + \|\mathbf{z}_v\|^2(4\epsilon)^{-1}\big)$$

and

$$\Omega_2(z_3, \tilde{\mathbf{p}}, \tilde{\mathbf{v}}, \tilde{f}_\omega) = \Omega_2(z_3, \mathbf{z}_{v1}, \mathbf{z}_{v2}, z_{\omega 3})$$
$$= -(1 + k_1 k_2)\lambda_v^{-1}z_3\mathbf{u}_2^\top \mathbf{R}^\top \mathbf{z}_{v2} - (\zeta_v\lambda_v + 3k_1 + 3k_2)$$
$$\times z_3\mathbf{u}_2^\top \mathbf{R}^\top \mathbf{z}_{v1} - z_3\delta_1 z_{\omega 3}$$
$$\leq (1 + k_1 k_2)\lambda_v^{-1}\big(\epsilon\|z_3\|^2 + \|\mathbf{z}_v\|^2(4\epsilon)^{-1}\big)$$
$$+ (\zeta_v\lambda_v + 3k_1 + 3k_2)\big(\epsilon\|z_3\|^2 + \|\mathbf{z}_v\|^2(4\epsilon)^{-1}\big)$$
$$+ |\delta_1|\big(\epsilon\|z_3\|^2 + \|\mathbf{z}_v\|^2(4\epsilon)^{-1}\big).$$

Then, we can rewrite (15) as

$$\dot{V}_4 \leq -\vartheta_1\|\mathbf{z}_1\|^2 - \vartheta_2\|\mathbf{z}_2\|^2 - \vartheta_3\|z_3\|^2 - \vartheta_4\|\mathbf{z}_v\|^2 - \vartheta_5\|\mathbf{z}_\omega\|^2 + \vartheta \leq -\vartheta_{\min}\big(\|\mathbf{z}\|^2 - \vartheta\vartheta_{\min}^{-1}\big) \quad (16)$$

where $\mathbf{z} = [\|\mathbf{z}_1\|, \|\mathbf{z}_2\|, \|z_3\|, \|\mathbf{z}_v\|, \|\mathbf{z}_\omega\|]^\top$ and

$$\vartheta_{\min} = \min\{\vartheta_1, \vartheta_2, \vartheta_3, \vartheta_4, \vartheta_5\}$$

with $\vartheta_1 = k_1 - \epsilon, \vartheta_2 = k_2 - 3\epsilon - k_1\epsilon\lambda_v^{-1}, \vartheta_3 = k_3 - (1 + k_1 k_2)\epsilon\lambda_v^{-1} - (\zeta_v\lambda_v + 3k_1 + 3k_2)\epsilon - \|\delta_1\|\epsilon, \vartheta_4 = \lambda_v - (1 + k_1 k_2)(4\lambda_v\epsilon)^{-1} - (\zeta_v\lambda_v + 3k_1 + 3k_2)(4\epsilon)^{-1} - (1 + k_1)(4\lambda_v\epsilon)^{-1} - 3(4\epsilon)^{-1} - 2\lambda_{\max}(\mathbf{Q}_v)\epsilon, \vartheta_5 = \lambda_\omega - 2\lambda_{\max}(\mathbf{Q}_\omega)\epsilon - \|\delta_1\|(4\epsilon)^{-1}, \vartheta = \|\delta\|^2(4\epsilon)^{-1} + 2\lambda_{\max}(\mathbf{Q}_v)\bar{f}_v^2(4\epsilon)^{-1} + 2\lambda_{\max}(\mathbf{Q}_\omega)\bar{f}_\omega^2(4\epsilon)^{-1}$ and ϵ is an arbitrarily positive number. Control parameters are chosen such that $\vartheta_i (i = 1, 2, \ldots, 5)$ is positive.

From (16), we have $\dot{V}_4$ is strictly negative definite for $\|\mathbf{z}\| > (\vartheta\vartheta_{\min}^{-1})^{\frac{1}{2}}$. It follows that $\|\mathbf{z}\|$ is uniformly bounded by $(\vartheta\vartheta_{\min}^{-1})^{\frac{1}{2}}$, which can be made as small as possible by tuning the control parameters.

6. EXPERIMENTAL RESULTS

Experimental test was conducted in the Sensor-based Cooperative Robotics Research Lab, University of Macau. The vehicle used for the experimental test is a radio-controlled hovercraft, as depicted in Fig. 1, which is low-cost and highly maneuverable. Due to the lack of payload for on-board sensors, we use a motion capture system VICON, together with markers attached on the vehicle, to measure the state of the hovercraft, including the position, orientation, linear and angular velocity, with the linear velocity measurement being used only as ground truth. The measured position, orientation and angular velocity of the hovercraft are fed back into the controller running in the Simulink/Matlab, as shown in Fig. 3. The actuation signals, thrust force and rudder angle, are sent to the hovercraft at the maximum rate the radio link allows, i.e., 45 Hz. The nonidealities introduced by the sampling rate limitation, together with any delays existing in the network and computer architecture, are negligible with respect to the slow dynamics of the physical actuators (motors) in the vehicle system. For more details about experimental setup, the reader is referred to Xie et al. (2019).
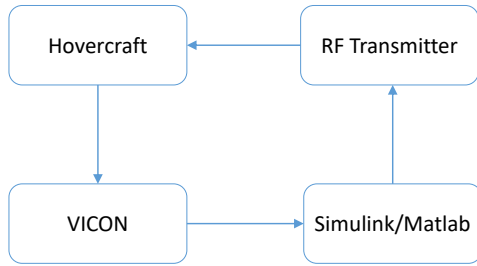
Fig. 3. Control architecture.

The reference trajectory is an ellipse described by

$$\mathbf{p}_d(t) = \left(\begin{bmatrix} d_x \cos(r_x t) \\ d_y \sin(r_y t) \end{bmatrix} - \begin{bmatrix} 0 \\ 0.2 \end{bmatrix} \right) \text{(m)}$$

where $d_x = 1.1, d_y = 1.2, r_x = r_y = 1.0$. The parameters used in the test are given as: $m = 0.5(\text{kg}), J = 0.008(\text{kg} \cdot \text{m}^2), k_1 = 2, k_2 = 1, k_3 = 1, \boldsymbol{\delta} = [-0.15, 0]^\top, \lambda_v = 30, \lambda_\omega = 30, \zeta_v = 0.1 \times 10^{-1}, \zeta_\omega = 0.2 \times 10^{-2}$.

The contrast of the actual trajectory described by the vehicle and desired trajectory is depicted in Fig. 4, from where we can conclude that the vehicle tracks the desired trajectory closely. Correspondingly, Fig. 5 displays the time evolution of $\|\mathbf{z}_1\|$, $\|\mathbf{z}_2\|$ and $\|z_3\|$ obtained from the simulation and experimental tests. Notice that compared with the simulation results, the performance of the controller is degraded in the experimental test (with larger tracking errors), which can be attributed to the fact that the issued commands are not perfectly followed by the vehicle due to unmodeled actuator dynamics, erroneous identification, linear velocity estimation error, etc. In steady state, the error statistics of the tracking errors obtained from the experimental test are given in Table 2. The comparison of the measured linear velocity $\mathbf{v}$ (obtained from VICON) and the estimated linear velocity $\hat{\mathbf{v}}$ is given in Fig. 6, from where we can

Table 2. Root mean square error (RMSE) and standard deviation (SD)

Error	RMSE	SD	Unit
$\|\mathbf{z}_1\|$	0.160	0.030	m
$\|\mathbf{z}_2\|$	0.209	0.063	m/s
$\|z_3\|$	1.3	0.2	rad/s

also see the estimation error $\|\tilde{\mathbf{v}}\|$ is driven to the neighborhood of zero, whose RMSE and SD are 0.052(m/s) and 0.021(m/s), respectively. Fig. 7 displays the time evolution of estimated disturbances $\hat{\mathbf{f}}_v$, $\mathbf{R}^\top\hat{\mathbf{f}}_v$ (expressed in the body frame) and $\hat{f}_\omega$. Notice that the estimated $\hat{\mathbf{f}}_v$ presents some periodic ripples, whose period is almost the same as the period of the reference trajectory, showing that $\hat{\mathbf{f}}_v$ is estimating the vehicle's unmodeled dynamics. Moreover, $\hat{f}_\omega$ converges to a neighborhood of a constant -0.5, which is reasonable if we consider the fact that the desired angular velocity of the vehicle is a constant, validating that $\hat{f}_\omega$ is estimating the vehicle's unmodeled dynamics associated with the vehicle's angular velocity.
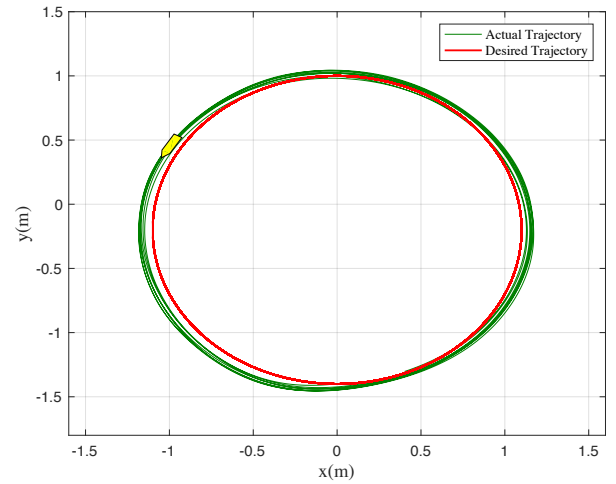
Fig. 4. Time evolution of the hovercraft's actual trajectory and desired ellipse trajectory in steady state.
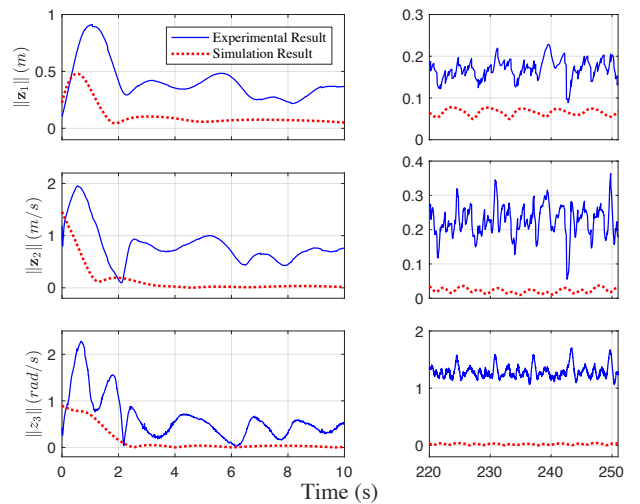
Fig. 5. The time evolution of the position error $\|\mathbf{z}_1\|$, linear velocity error $\|\mathbf{z}_2\|$, angular velocity error $\|z_3\|$ obtained from the simulation and experimental tests.
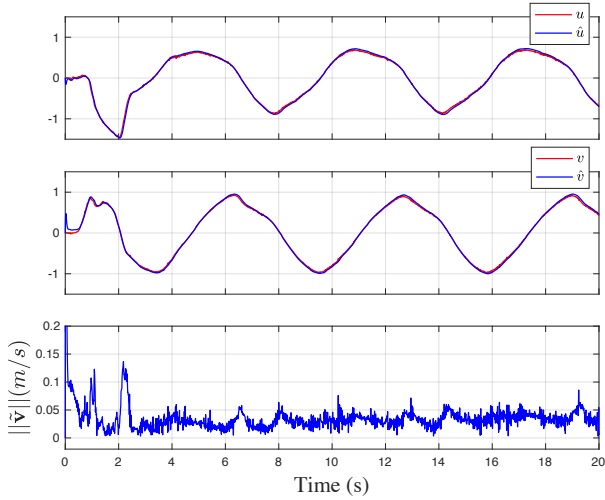
Fig. 6. Comparison of the measured $\mathbf{v}$ and the estimated $\hat{\mathbf{v}}$, with the time evolution of the estimation error $\|\tilde{\mathbf{v}}\|$.
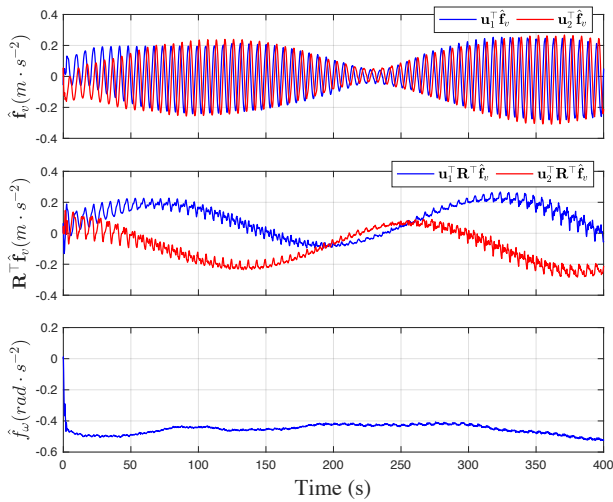

Fig. 7. The time evolution of $\hat{\mathbf{f}}_v$, $\mathbf{R}^\top\hat{\mathbf{f}}_v$ and $\hat{f}_\omega$.

7. CONCLUSION

This paper presented a solution to the problem of trajectory tracking for an underactuated hovercraft with unmeasured linear velocity and subject to disturbances, guaranteeing the vehicle can be stabilized along with a neighborhood of a reference trajectory. To achieve robust performance, nonlinear observers for unmeasured linear velocity and unknown disturbances are designed. Experimental results were given to validate the efficiency of the proposed control strategy.

REFERENCES

Aguiar, A.P., Cremean, L., and Hespanha, J.P. (2003). Position tracking for a nonlinear underactuated hovercraft: controller design and experimental results. In *42nd IEEE International Conference on Decision and Control*, volume 4, 3858–3863.

Aguiar, A.P. and Hespanha, J.P. (2007). Trajectory-tracking and path-following of underactuated autonomous vehicles with parametric modeling uncertainty. *IEEE Transactions on Automatic Control*, 52(8), 1362–1379.

Belleter, D., Maghenem, M.A., Paliotta, C., and Pettersen, K.Y. (2019). Observer based path following for underactuated marine vessels in the presence of ocean currents: A global approach. *Automatica*, 100, 123 – 134.

Cabecinhas, D., Batista, P., Oliveira, P., and Silvestre, C. (2018). Hovercraft control with dynamic parameters identification. *IEEE Transactions on Control Systems Technology*, 26(3), 785–796.

Cabecinhas, D. and Silvestre, C. (2019). Trajectory tracking control of a nonlinear autonomous surface vessel. In *2019 American Control Conference (ACC)*, 4380–4385.

Do, K. and Pan, J. (2006). Global robust adaptive path following of underactuated ships. *Automatica*, 42(10), 1713 – 1722.

Grovlen, A. and Fossen, T.I. (1996). Nonlinear control of dynamic positioned ships using only position feedback: an observer backstepping approach. In *Proceedings of 35th IEEE Conference on Decision and Control*, volume 3, 3388–3393.

Li, Z., Sun, J., and Oh, S. (2009). Design, analysis and experimental validation of a robust nonlinear path following controller for marine surface vessels. *Automatica*, 45(7), 1649 – 1658.

Liu, L., Wang, D., and Peng, Z. (2019). State recovery and disturbance estimation of unmanned surface vehicles based on nonlinear extended state observers. *Ocean Engineering*, 171, 625 – 632.

Loueipour, M., Keshmiri, M., Danesh, M., and Mojiri, M. (2015). Wave filtering and state estimation in dynamic positioning of marine vessels using position measurement. *IEEE Transactions on Instrumentation and Measurement*, 64(12), 3253–3261.

Lu, D., Xie, W., Cabecinhas, D., Cunha, R., and Silvestre, C. (2019). Path following controller design for an underactuated hovercraft with external disturbances. *19th International Conference on Control, Automation and Systems*.

Perera, L.P. and Soares, C.G. (2012). Pre-filtered sliding mode control for nonlinear ship steering associated with disturbances. *Ocean Engineering*, 51, 49 – 62.

Reyhanoglu, M. (1997). Exponential stabilization of an underactuated autonomous surface vessel. *Automatica*, 33(12), 2249 – 2254.

Xie, W., Cabecinhas, D., Cunha, R., and Silvestre, C. (2019). Robust motion control of an underactuated hovercraft. *IEEE Transactions on Control Systems Technology*, 27(5), 2195–2208.

Yang, Y., Du, J., Liu, H., Guo, C., and Abraham, A. (2014). A trajectory tracking robust controller of surface vessels with disturbance uncertainties. *IEEE Transactions on Control Systems Technology*, 22(4), 1511–1518.

Yin, S. and Xiao, B. (2017). Tracking control of surface ships with disturbance and uncertainties rejection capability. *IEEE/ASME Transactions on Mechatronics*, 22(3), 1154–1162.

Zhao, Z. and Guo, B. (2015). Extended state observer for uncertain lower triangular nonlinear systems. *Systems & Control Letters*, 85, 100 – 108.